fields seen by the electrons. To obtain the experimental cross section, one must solve the usual boundary value problem at the metal surface. This will introduce Fresnel correction factors which are, however, of the order of unity.[11]

In conclusion, we point out that the proposed light scattering experiment with its inherently good energy resolution can be utilized to give a much better value for the gap parameter $2g(T)$, although it does not determine $\mathbf{Q}$.

PHYSICAL REVIEW VOLUME 182, NUMBER 3 15 JUNE 1969

Dispersion of Ordinary and Extraordinary High-Frequency Waves in Metals

E-Ni Foo*
Bell Telephone Laboratories, Murray Hill, New Jersey 07974
(Received 23 December 1968)

This paper is an extended discussion of the dispersion curves of the high-frequency waves (HFW) occurring in simple metals near the Azbel-Kaner cyclotron resonances. The conductivity $\sigma(\mathbf{k},\omega,\omega_c)$ for the case of a general ellipsoidal Fermi surface is derived, and the spherical and cylindrical Fermi surfaces are then treated as limiting cases. Numerical calculations of the dispersion curves of both ordinary and extraordinary HFW, for the case of a spherical Fermi surface, are evaluated over a range of wavelengths that bridges the long-wavelength limit, which has been observed experimentally, and the short-wavelength limit, which was predicted by Kaner and Skobov. The dispersion curves show oscillatory characteristics at intermediate wavelengths. The oscillatory character manifests itself most strongly for the case of a cylindrical Fermi surface, where its physical origin becomes apparent.

I. INTRODUCTION

RECENTLY, new electromagnetic modes which can propagate in simple metals near the Azbel-Kaner cyclotron resonances (AKCR) have been observed[1,2] and are referred to as high-frequency waves (HFW). The existence of these HFW in metals was first discussed by Kaner and Skobov.[3] Their predictions were confined to the short-wavelength limit ($kR \gg 10^2$, where $R = V_F/\omega$); however, the experimentally observed HFW modes are found in the long-wavelength limit ($0 \leqslant kR \lesssim 10$). An extensive theoretical discussion for the latter regime has been given by Platzman, Walsh, and Foo[4] (PWF) for the case of the ordinary mode ($\mathbf{E} \| \mathbf{B}$). In this paper we derive a general expression for the conductivity in the case of a general ellipsoidal Fermi surface (FS), which can be reduced to the spherical or cylindrical cases by taking proper limits. We present complete dispersion curves of both ordinary and extraordinary modes ($\mathbf{E} \perp \mathbf{B}$) for the case of a spherical free-electron FS over a large range of wavelengths ($0 < kR < 100$). In the intermediate-wavelength regime, $5 < kR < 30$, the dispersion curves exhibit an oscillatory behavior which is especially strong for the extraordinary mode in the spherical FS case. We then show that this behavior is even more pronounced in the case of a cylindrical FS, which has not only a constant effective mass but also a constant cyclotron radius. The extraordinary HFW dispersion curves for a cylindrical FS in the $0 < kR < 8$ regime are evaluated and compared with those for the spherical FS. The origin of the oscillatory characteristics is emphasized.

II. CONDUCTIVITY TENSOR OF AN ELLIPSOIDAL FS

We wish to calculate the wave vector and frequency-dependent magnetoconductivity tensor $\sigma_{ij}(\mathbf{k},\omega)$ for a general ellipsoidal sheet of FS arbitrarily oriented in a magnetic field $\mathbf{B}$ ($\hat{z}$ axis). The FS is defined by the energy-momentum relation

$$E = (2m_0)^{-1} \sum \alpha_{ij} P_i P_j , \tag{1}$$

where m_0 is the free-electron mass, and α_{ij} is the normalized inverse effective-mass tensor, which is symmetric. We use the form of expression originated by Overhauser and Rodriquez[5] for the magnetoconductivity of an arbitrary Fermi distribution of noninteracting electrons:

$$\sigma_{ij} = \frac{2e^3 B}{h^3 C} \int dE \left(-\frac{df_0}{dE} \right) \int dP_z \, T(E,P_z) \sum_{n=-\infty}^{\infty} v_{ni} v_{nj}^* \times \{ 1/\tau + i[\omega - 2\pi n/T(E,P_z) - \mathbf{k}\cdot\mathbf{v}_s] \}^{-1} . \tag{2}$$

* Present address: City College of the City University of New York.

[1] W. M. Walsh, Jr., and P. M. Platzman, Phys. Rev. Letters **15**, 784 (1965).

[2] P. M. Platzman and W. M. Walsh, Jr., Phys. Rev. Letters **19**, 514 (1967); **20**, 89(E) (1968).

[3] E. A. Kaner and V. G. Skobov, Fiz. Tverd. Tela **6**, 1104 (1964) [English transl.: Soviet Phys.—Solid State **6**, 851 (1964)].

[4] P. M. Platzman, W. M. Walsh, Jr., and E-Ni Foo, Phys. Rev. **172**, 689 (1968).

[5] A. W. Overhauser and S. Rodriquez, Phys. Rev. **141**, 431 (1966).

Here $T(E,P_z)$ is the cyclotron period of an electron of energy E and crystal momentum P_z along $\mathbf{B}$. The vector $\mathbf{v}_n$ where n is integer is given by

$$\mathbf{v}_n(E,P_z)=\frac{1}{T}\int_0^T du\,\mathbf{v}(E,P_z,u)\times\exp\left[i\mathbf{k}\cdot\mathbf{R}_p(E,P_z,u)-\frac{2\pi i n u}{T}\right], \quad (3)$$

where the timelike parameter u specifies the electron's position on the orbit defined by E and P_z. The quantity $\mathbf{v}(E,P_z,u)$ is the electron's velocity and $\mathbf{R}_p(E,P_z,u)$ describes the periodic part of its spatial motion. A phenomenological scattering time τ is used to relax the distribution function to equilibrium but will, in fact, be neglected in the final computations.

For an ellipsoidal FS, the effective-mass ratio is

$$m^*=m_0/(\alpha_{xx}\alpha_{yy}-\alpha_{xy}^2)^{1/2}, \quad (4)$$

and the cyclotron frequency $\omega_c=eB/m^*C$ and the period $T=2\pi/\omega_c$ are independent of P_z. The velocity components are

$$\begin{aligned}v_x&=(P_z/m_0)(\alpha_{xx}\gamma_x\cos\omega_c u+\alpha_{xy}\gamma_y\sin\omega_c u),\\ v_y&=(P_z/m_0)(\alpha_{yx}\gamma_x\cos\omega_c u+\alpha_{yy}\gamma_y\sin\omega_c u),\\ v_z&=(P_z/m_0)(\gamma_z+\alpha_{zx}\gamma_x\cos\omega_c u+\alpha_{zy}\gamma_y\sin\omega_c u),\end{aligned} \quad (5)$$

where

$$\begin{aligned}\gamma_x&=[2(\alpha_{yy})^{1/2}/(\alpha_{yx}^2-\alpha_{xx}\alpha_{yy})][(2m_0E/P_z^2)\\ &\quad\times(\alpha_{xx}\alpha_{yy}-\alpha_{xy}^2)+(\alpha_{yy}\alpha_{xz}^2+\alpha_{zz}\alpha_{yx}^2+\alpha_{xx}\alpha_{yz}^2\\ &\quad-\alpha_{xx}\alpha_{yy}\alpha_{zz}-2\alpha_{xy}\alpha_{yz}\alpha_{zx})]^{1/2},\\ \gamma_y&=[2(\alpha_{xx})^{1/2}/(\alpha_{yx}^2-\alpha_{xx}\alpha_{yy})][(2m_0E/P_z^2)\\ &\quad\times(\alpha_{xx}\alpha_{yy}-\alpha_{xy}^2)+(\alpha_{yy}\alpha_{xz}^2+\alpha_{zz}\alpha_{yx}^2+\alpha_{xx}\alpha_{yz}^2\\ &\quad-\alpha_{xx}\alpha_{yy}\alpha_{zz}-2\alpha_{xy}\alpha_{yz}\alpha_{zx})]^{1/2},\\ \gamma_z&=(\alpha_{yx}^2-\alpha_{xx}\alpha_{yy})^{-1}(2\alpha_{zx}\alpha_{xy}\alpha_{yz}+\alpha_{zz}\alpha_{yx}^2-\alpha_{yy}\alpha_{zx}^2\\ &\quad+\alpha_{xx}\alpha_{zy}^2-\alpha_{xx}\alpha_{yy}\alpha_{zz}).\end{aligned} \quad (6)$$

For detailed evaluation we consider the case of $\mathbf{k}$ parallel to the x axis. The x component of $\mathbf{v}_s$ is then equal to zero. By substituting Eqs. (4) and (5) into Eq. (2) and integrating over E, we obtain

$$\sigma_{ij}=\sum_{l,m=x,y}T_{ij}{}^{lm}\sigma_{lm}{}^0+\delta_{iz}\delta_{jz}\sigma_{zz}{}^0, \quad i,j=x,y,z \quad (7)$$

where

$$T_{ij}{}^{lm}=\alpha_{li}\alpha_{mj} \quad (8)$$

and

$$\sigma_{zz}{}^0=\frac{N_0}{i}\sum_{n=-\infty}^{\infty}\int\frac{J_n{}^2(b)}{\omega-n\omega_c}\gamma_z{}^2P_z{}^2dP_z, \quad (9)$$

$$\sigma_{xx}{}^0=\frac{N_0}{i}\sum_{n=-\infty}^{\infty}\int\frac{n^2J_n{}^2(b)}{b^2(\omega-n\omega_c)}\gamma_x{}^2P_z{}^2dP_z, \quad (10)$$

$$\sigma_{yy}{}^0=\frac{N_0}{i}\sum_{n=-\infty}^{\infty}\int\frac{[J_n{}'(b)]^2}{\omega-n\omega_c}\gamma_y{}^2P_z{}^2dP_z, \quad (11)$$

$$\sigma_{xy}{}^0=-\sigma_{yx}{}^0=N_0\sum_{n=-\infty}^{\infty}\int\frac{nJ_n(b)J_n{}'(b)}{b(\omega-n\omega_c)}\gamma_x\gamma_yP_z{}^2dP_z, \quad (12)$$

and the constant

$$N_0=4\pi e^3B/h^3cm_0{}^2\omega_c, \quad (13)$$

and the $J_n(b)$ and $J_n{}'(b)$ are Bessel functions and their derivatives with argument

$$b=kc\gamma_yP_z/eB. \quad (14)$$

For a spherical FS, $\alpha_{ij}=\delta_{ij}$ and then Eq. (7) reduces to the well-known expression for the magnetoconductivity.[6-8] In this case $b=kR_c\sin\theta$, where $R_c=V_F/\omega_c$ and θ is the angle between $\mathbf{B}$ and $\mathbf{V}_F$. For a cylindrical FS with $\mathbf{B}$ parallel to its axis, $b=kR_c$ and is independent of θ. In both cases, σ_{xz} and σ_{yz} are equal to zero by symmetry.

III. HFW DISPERSION RELATION

To discuss the dispersion behavior of the HFW, we ignore the complete boundary-value problem,[4] i.e., the coupling or excitation problem, and concentrate on the bulk dielectric properties of the metal. For propagation accurately perpendicular to the magnetic field, the HFW are undamped as long as ordinary collisions are neglected ($\tau\equiv\infty$). Defining $\mathbf{z}\|\mathbf{B}$ and $\mathbf{x}\|\mathbf{k}$ the off-diagonal components of the conductivity tensor $\sigma_{xz}=\sigma_{zx}$ and $\sigma_{yz}=-\sigma_{zy}$ vanish. In this case, the solution of Maxwell's equations yields the familiar dispersion relation

$$(k^2/k_0{}^2-\epsilon_{zz})[k^2/k_0{}^2-(\epsilon_{yy}+\epsilon_{xy}/\epsilon_{xx}{}^2)]=0, \quad (15)$$

where the dielectric tensor

$$\epsilon_{\alpha\beta}(\mathbf{k},\omega)=\delta_{\alpha\beta}-4\pi\sigma_{\alpha\beta}(\mathbf{k},\omega,\mathbf{B})/i\omega. \quad (16)$$

Here $k_0=\omega/c$, ω is the frequency of the HFW, and c the speed of light. The first term $\delta_{\alpha\beta}$ is the displacement current and the second term is a complex tensor contribution due to the magnetized conduction electrons. The first root,

$$k^2/k_0{}^2=\epsilon_{zz}, \quad (17)$$

[6] M. Cohen, M. Harrison, and W. Harrison, Phys. Rev. **117**, 937 (1960).
[7] S. J. Buchsbaum and P. M. Platzman, Phys. Rev. **154**, 395 (1967).
[8] S. G. Eckstein, Bull. Am. Phys. Soc. **9**, 550 (1964).

is the so-called "ordinary wave" for which $\mathbf{E}\|\mathbf{z}$, a purely transverse mode. It will be discussed in Sec. III A. The other root,

$$k^2/k_0^2=\epsilon_{yy}+\epsilon_{xy}^2/\epsilon_{xx}, \tag{18}$$

is known as the "extraordinary wave," which will be discussed in Sec. III B. This mode is not purely transverse but has a weak longitudinal component.

In the range of parameters where the HFW are observed one has $\omega_p^2/\omega_c^2\sim10^{10}\gg k^2/k_0^2\sim10^5\gg1$. Because of the extremely high plasma frequency in metals, the response due to the conduction electrons is dominant, so that one can neglect the contribution due to the displacement current in Eq. (16). Since we are interested in the regime of $kR\sim100$, i.e., $\omega_p^2/\omega_c^2\sim k^2/k_0^2$, we must keep the term k^2/k_0^2 in computing the dispersion relations.

A. Ordinary Wave

In this section we consider the dispersion behavior of the ordinary wave in potassium which most closely approximates the nearly-free-electron model. The numerically computed solution of Eq. (17) in the fundamental cyclotron resonance region, i.e., $\omega_c\gtrsim\omega$, with $\omega_p\sim6\times10^{15}$ rad/sec, the microwave frequency $\omega=7.5\times10^{10}$ rad/sec, and $V_F/c=3\times10^{-3}$ is shown in Fig. 1. For $kR\lesssim10$, its behavior was discussed extensively by PWF.[4] Here we extend the dispersion curve to large values of $kR\sim100$. We find that the dispersion curve bridges the long-wavelength limit, i.e., $kR\sim1$, which has been observed experimentally and the short-wavelength limit which was predicted by Kaner and Skobov.[3] For $kR\gg1$, the asymptotic solutions of the dispersion curves[3] are determined by

$$(\omega_p^2/\omega_c^2)\cot(\pi\omega/\omega_c)+k^3R/k_0^2=0. \tag{19}$$

They approach monotonically to the axis $\omega_c/\omega=n$, as kR increases. For the fundamental branch, it begins to bend back and approaches monotonically the $\omega_c/\omega=1$ axis, as $kR\lesssim30$. The oscillatory intermediate behavior will be discussed below.

B. Extraordinary Wave

The dispersion curves of the extraordinary HFW were computed numerically using Eq. (18) in the regions of the first three cyclotron resonances, as shown in Fig. 2. The characteristics of the extraordinary wave differ from those of the ordinary wave in several respects. There are two branches of HFW originating from each cyclotron resonance except at the fundamental where only one branch exists. For $kR\ll1$, the dispersion curves of the extraordinary waves are determined to lowest order by

$$\frac{(kR_c)^{2l+2}}{(\omega/\omega_c)^2-l^2}+2^{2l+2}(l-1)!(l+1)!\frac{C_0C_{2l-2}}{C_{2l+2}C_{2l-2}-C_{2l}^2}=0, \quad l\gtrsim1 \tag{20}$$

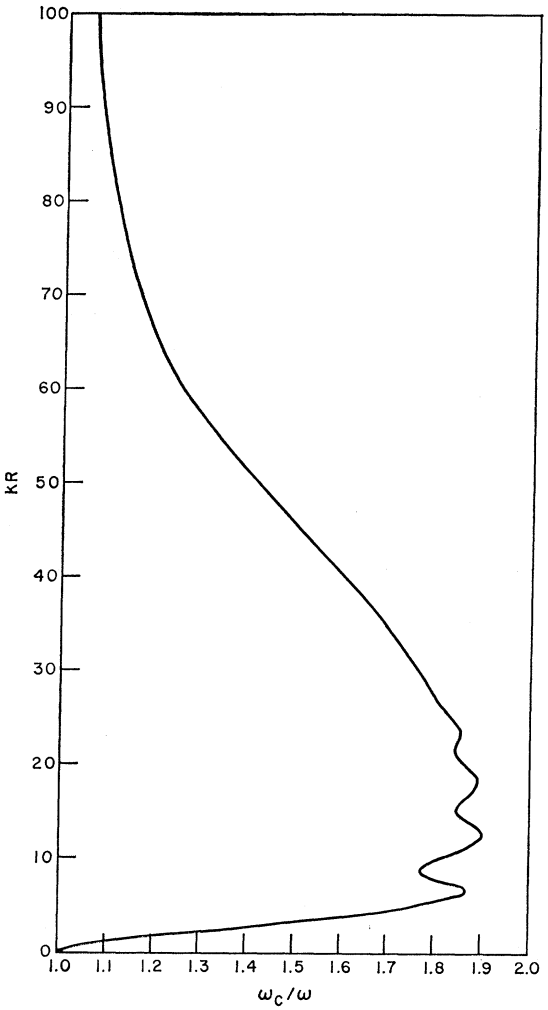

FIG. 1. Dispersion curve of the ordinary HFW, with $\omega_p\sim6\times10^{15}$ rad/sec, $\omega=7.5\times10^{10}$ rad/sec, and $V_F/c=3\times10^{-3}$.

and

$$\frac{(kR_c)^{2l-2}}{(\omega/\omega_c)^2-l^2}+\frac{2^{2l-3}(l-1)!(l-2)!C_0}{lC_{2l-2}}, \quad l\gtrsim2 \tag{21}$$

where

$$C_{2l}=2\int_0^{\pi/2}\sin^{2l+3}\theta d\theta =2\times\frac{2\times4\times\cdots\times(2l+2)}{1\times3\times5\times\cdots\times(2l+3)}, \tag{22}$$

and l denotes the order of the region under consideration, i.e., $l>\omega/\omega_c>l-1$. We call the solution of Eq. (20) the higher mode ω_l^+, which is proportional to $(kR_c)^{2l+2}$, and that of Eq. (21) the lower mode ω_l^-, which is proportional to $(kR_c)^{2l-2}$. The latter modes first appear (ω_1^- does not exist) for $l=2$, with a quadratic kR_c dependence

$$\frac{(kR_c)^2}{(\omega/\omega_c)^2-4}+\frac{5}{4}=0. \tag{23}$$

The higher mode ω_1^+, which is the only mode appearing in the fundamental cyclotron resonance regime, is determined by

$$\frac{(kR_c)^4}{(\omega/\omega_c)^2-1}+350=0. \tag{24}$$

This mode has a very strong oscillatory character for finite kR. The periodicity in kR is very clear and the slope reversals are very sharp compared to the slightly oscillatory behavior of the ordinary wave. In the regime $\omega_c/\omega>1$, ω_1^+ is multiple-valued in the range $1.4<\omega_c/\omega<2.9$, i.e., for a given magnetic field several waves of distinct k may be excited.

Experimentally, the HFW are observed to produce oscillations in the effective surface resistance of a thin metal slab carrying surface currents on both faces as the changing magnetic field causes the wavelength and, thus, the phase of the transmitted waves to vary. Under antisymmetric excitation conditions power-absorption minima occur when $\frac{1}{2}(2n+1)\lambda=L$, $n=0, 1, 2\cdots$, where $\lambda=2\pi/k$ is the wavelength in the metal and L is the sample thickness. In those regions of magnetic field where only a single long-wavelength branch of a dispersion curve exists, a "clean" surface resistance oscillation is observed and the dispersion may be unambiguously measured, e.g., in the range $1<\omega_c/\omega<1.4$ for the case of the extraordinary HFW. However, in regions where two or more dispersion-curve branches exist, corresponding to simultaneous excitation and propagation of two or more waves of differing phase velocities, more complex surface resistance changes are observed, e.g., for $1.4<\omega_c/\omega<2.9$ in the extraordinary HFW case. Beyond the final turning point of the dispersion curve ($\omega_c/\omega>2.9$) the metal is completely cut off. This is reflected experimentally by a modest change in the surface resistance.[4,9]

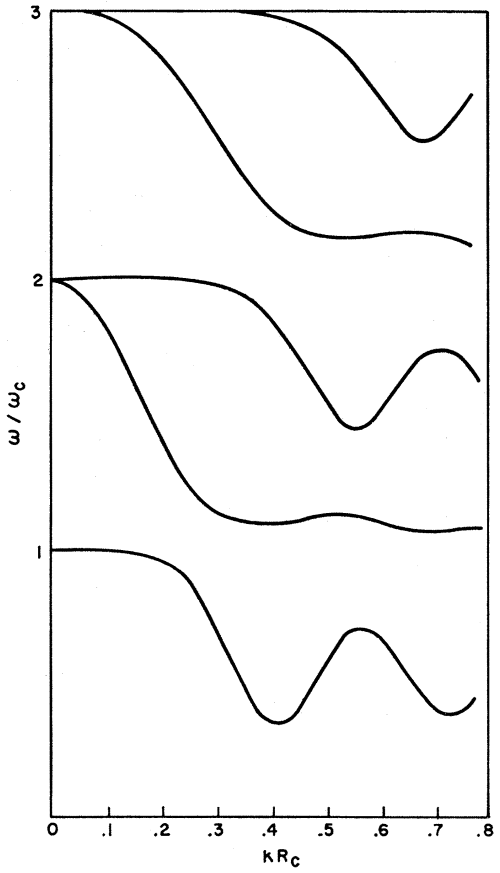

FIG. 3. Dispersion curve of the extraordinary wave as a function of ω/ω_c and kR_c, with $\omega_p\sim6\times10^{15}$ rad/sec, $\omega_c=7.5\times10^{10}$ rad/sec, and $V_F/c=3\times10^{-3}$.

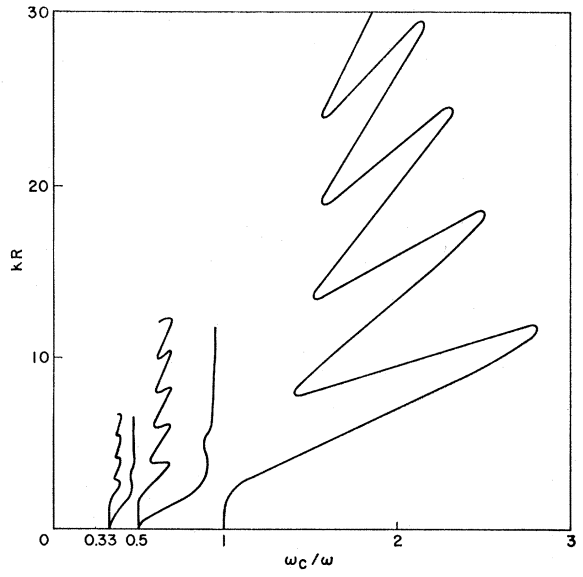

FIG. 2. Dispersion curve of the first three harmonics of the extraordinary wave as a function of kR and ω_c/ω, with $\omega_p\sim6\times10^{15}$ rad/sec, $\omega=7.5\times10^{10}$ rad/sec, and $V_F/c=3\times10^{-3}$.

In order to understand the oscillatory characteristics of the dispersion relations, it is convenient to examine the dispersion relation of the HFW using a slightly altered set of variables. We examine the solution of Eq. (18) as a function of kR_c and ω/ω_c. The transcribed dispersion curves are shown in Fig. 3 as the solid lines. One notices that the oscillatory periodicity in kR_c is approximately equal to π. The oscillatory modes ω_l^+ for $l\geqslant2$ are analogous to ω_1^+, except that the first slope-reversal points are shifted upward by $\frac{1}{2}\pi$ as l increases by 1.

The oscillatory behavior manifests itself even more strikingly for **B** parallel to the axis of a cylindrical FS, for which the cyclotron radius R_c is independent of P_z. The argument b of the Bessel functions in the conduc-

[9] W. M. Walsh, Jr. (private communication).

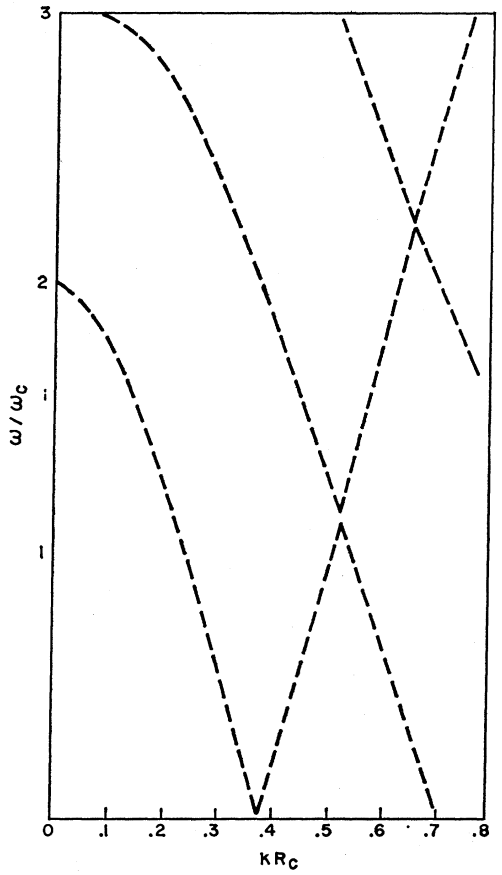

FIG. 4. Dispersion curve of the extraordinary wave for the case of a cylindrical (FS) as a function of ω/ω_c and kR_c.

tivity tensor [Eqs. (9)–(13)] then reduces to kR_c and one can factor the Bessel functions out of the integrals. Therefore, the oscillatory behavior of HFW for a cylindrical FS should reflect just the periodicity of the Bessel functions. The numerically computed dispersion curves for the cylindrical case are plotted in Fig. 4 as a function of kR_c and ω/ω_c. One notices that the periodicity is most clear and the slope reversals are extremely sharp for the cylindrical case. For example, near $\omega/\omega_c=0$, the slope reverses at $kR_c=3.8317$, 7.0156, $\cdots$, etc., which coincide with the zeros of J_0'. The slight shift of the periodicity and the more gradual slope reversals in the case of the spherical FS are due to the averaging over different cyclotron radii.

We should also like to point out that for the cylindrical case, the lower modes ω_l^- are the only set of nontrivial solutions of Eq. (18) in the long-wavelength regime, and the higher modes, which are reduced to $\omega_l^+=l\omega_c$, are trivial solutions which have no physical significance.

Since the cyclotron orbit radii are the same for all electrons on the cylindrical FS, we can treat this problem by considering the motion of a single electron only. Consider an electron of velocity $\mathbf{V}_F$ moving in a plane perpendicular to a magnetic field ($\mathbf{B}\|z$ axis). Then we apply a weak external electromagnetic field $\varepsilon e^{i(\omega t-kx)+\delta t}$, which is treated as a perturbation. Here we turn on the electromagnetic field adiabatically by taking the limit of the response as δ goes to zero. The electromagnetic field will not be attenuated if no net energy current is transferred from the field to the electron during a cyclotron period. The x component of the electron's orbit is $x=R_c\sin\omega_c t$, and the electromagnetic field along the orbit is

$$\varepsilon\exp[(i\omega+\delta)(t-t_0)-ikR_c(\cos\omega_c t-\cos\omega_c t_0)], \quad (25)$$

with the appropriate initial condition at $t=t_0$. The net energy gained by the electron at time t_0 is

$$E(t_0)=e\int_{-\infty}^{t_0} dt\ \mathbf{v}\cdot\varepsilon\exp[(i\omega+\delta)(t-t_0) -ikR_c(\cos\omega_c t-\cos\omega_c t_0)]. \quad (26)$$

Then the net energy current $\mathbf{I}_E$ of an electron gas of density n during one cyclotron period T is

$$\mathbf{I}_E=n\int_0^T \mathbf{v}(t_0)E(t_0)dt_0 \quad (27)$$

$$=ne\int_0^T dt_0\,\mathbf{v}(t_0)\int_{-\infty}^{t_0} dt\ \mathbf{v}(t)\cdot\varepsilon\exp[(i\omega+\delta)(t-t_0) -ikR_c(\cos\omega_c t-\cos\omega_c t_0)], \quad (28)$$

where $\mathbf{v}(t)$ is the electron's velocity at time t, of which the x component is $V_F\cos\omega_c t$ and the y component is $V_F\sin\omega_c t$. The dispersion relation of the unattenuated electromagnetic wave can be obtained by solving

$$\mathbf{I}_E=0. \quad (29)$$

After carrying out the integrations and eliminating the parameter ε, one will obtain the same result as solving Eq. (18) for the cylindrical FS case. Since the integrand in Eq. (28) is a periodic function of t and t_0, one expects more than one value of kR_c which satisfies the condition (29). This means an electromagnetic wave of frequency ω can propagate through such a simple magnetized electron gas with multivalued wavelengths. This is the origin of the oscillatory behavior shown in the HFW dispersion curves.

ACKNOWLEDGMENTS

The author is grateful to Dr. P. M. Platzman and Dr. W. M. Walsh, Jr., for valuable discussions and suggestions about this work and their critical reading of the manuscript.